

Received Sept 1982 (61-1)

JOURNAL OF  
**NEUROPHYSIOLOGY**

- - - 680

January 1989  
Volume 61, Number 1

Neural Coding of Gustatory Information in the Thalamus of <i>Macaca mulatta</i> <i>T. C. Pritchard, R. B. Hamilton, and R. Norgren</i>	1
A Comparison of Supramammillary and Medial Septal Influences on Hippocampal Field Potentials and Single-Unit Activity <i>S. J. Y. Mizumori, B. L. McNaughton, and C. A. Barnes</i>	15
Modulation of a Steady-State $\text{Ca}^{2+}$ -Activated, $\text{K}^+$ Current in Tail Sensory Neurons of <i>Aplysia</i> : Role of Serotonin and cAMP <i>J. P. Walsh and J. H. Byrne</i>	32
An Evaluation of the Role of Identified Interneurons in Triggering Kicks and Jumps in the Locust <i>I. C. Gynther and K. G. Pearson</i>	45
W- and Y-Cells in the C Layers of the Cat's Lateral Geniculate Nucleus: Normal Properties and Effects of Monocular Deprivation <i>P. D. Spear, M. A. McCall, and N. Tumosa</i>	58
Deficits of Visual Attention and Saccadic Eye Movements After Lesions of Parieto-occipital Cortex in Monkeys <i>J. C. Lynch and J. W. McLaren</i>	74
Impulse Activity of a Crayfish Motoneuron Regulates Its Neuromuscular Synaptic Properties <i>G. A. Lnenicka and H. L. Atwood</i>	91
Cyclic AMP Selectively Reduces the N-Type Calcium Current Component of Mouse Sensory Neurons in Culture by Enhancing Inactivation <i>R. A. Gross and R. L. Macdonald</i>	97
Patterns of Spontaneous Discharge in Primate Spinothalamic Neurons <i>D. J. Surmeier, C. N. Honda, and W. D. Willis</i>	106
Electrical Properties and Innervation of Fibers in the Orbital Layer of Rat Extraocular Muscles <i>J. Jacoby, D. J. Chiarandini, and E. Stefani</i>	116
Somatotopic Organization of Forelimb Representation in Cervical Enlargement of Raccoon Dorsal Horn <i>B. H. Pubols, Jr., H. Hirata, and L. West-Johnsrud</i>	126
Spinocervical Tract Neurons Responsive to Light Mechanical Stimulation of the Raccoon Forepaw <i>H. Hirata and B. H. Pubols, Jr.</i>	138
Responses to Parallel Fiber Stimulation in the Guinea Pig Dorsal Cochlear Nucleus In Vitro <i>P. B. Manis</i>	149
A Voltage-Clamp Study of Isolated Stingray Horizontal Cell Non-NMDA Excitatory Amino Acid Receptors <i>T. J. O'Dell and B. N. Christensen</i>	162

(Continued)

Topographic and Directional Organization of Visual Motion Inputs for the Initiation of Horizontal and Vertical Smooth-Pursuit Eye Movements in Monkeys <i>S. G. Lisberger and T. A. Pavelko</i>	173
The Contribution of Articular Receptors to Proprioception With the Fingers in Humans <i>F. J. Clark, P. Grigg, and J. W. Chapin</i>	186
Cable Properties of Spinal Cord Motoneurons in Adult and Aged Cats <i>J. K. Engelhardt, F. R. Morales, J. Yamuy, and M. H. Chase</i>	194
Distribution of Combination-Sensitive Neurons in the Ventral Fringe Area of the Auditory Cortex of the Mustached Bat <i>H. Edamatsu, M. Kawasaki, and N. Suga</i>	202
Force Output of Cat Motor Units Stimulated With Trains of Linearly Varying Frequency <i>S. A. Binder-Macleod and H. P. Clamann</i>	208
Measurement of Passive Membrane Parameters With Whole-Cell Recording From Neurons in the Intact Amphibian Retina <i>P. A. Coleman and R. F. Miller</i>	218
Announcements	231



#### IMPORTANT CHANGE

As of July 1, 1989, the reference style for the *Journal of Neurophysiology* is changing in text from serial numbering to author's name and date. The unnumbered reference list should continue to be arranged alphabetically by author. See Information for Contributors for details and examples. It will be appreciated if authors of manuscripts submitted under the old system can make these changes during revision.

# JOURNAL OF NEUROPHYSIOLOGY

February 1989  
Volume 61, Number 2

- Long-Lasting Reduction of Excitability by a Sodium-Dependent Potassium Current  
in Cat Neocortical Neurons

*P. C. Schwindt, W. J. Spain, and W. E. Crill* 233

- Norepinephrine Selectively Reduces Slow  $\text{Ca}^{2+}$ - and  $\text{Na}^+$ -Mediated  $\text{K}^+$  Currents in  
Cat Neocortical Neurons

*R. C. Foehring, P. C. Schwindt, and W. E. Crill* 245

- Temporal Coding of Envelopes and Their Interaural Delays in the Inferior  
Colliculus of the Unanesthetized Rabbit

*R. Batra, S. Kuwada, and T. R. Stanford* 257

- Monaural and Binaural Response Properties of Neurons in the Inferior Colliculus  
of the Rabbit: Effects of Sodium Pentobarbital

*S. Kuwada, R. Batra, and T. R. Stanford* 269

- Kinetic Analysis of Acetylcholine-Induced Current in Isolated Frog Sympathetic  
Ganglion Cells

*N. Akaike, N. Tokutomi, and H. Kijima* 283

- A Differential Synaptic Input to the Motor Nuclei of Triceps Surae From the  
Caudal and Lateral Cutaneous Sural Nerves

*L. A. LaBella, J. P. Kehler, and D. A. McCrea* 291

- Inositol Trisphosphate and Activators of Protein Kinase C Modulate Membrane  
Currents in Tail Motor Neurons of *Aplysia*

*M. Sawada, L. J. Cleary, and J. H. Byrne* 302

- Thalamocortical Response Transformation in the Rat Vibrissa/Barrel System

*D. J. Simons and G. E. Carvell* 311

- Mnemonic Coding of Visual Space in the Monkey's Dorsolateral Prefrontal Cortex

*S. Funahashi, C. J. Bruce, and P. S. Goldman-Rakic* 331

- Input-Output Relationships of the Primary Face Motor Cortex in the Monkey  
(*Macaca fascicularis*)

*C.-S. Huang, H. Hiraba, and B. J. Sessle* 350

- Trifluoperazine Blocks GABA-Gated Chloride Currents in Cultured Chick Spinal  
Cord Neurons

*J. Yang and C. F. Zorumski* 363

- Differential Effects of Baclofen on Sustained and Transient Cells in the Mudpuppy  
Retina

*M. M. Slaughter and S.-H. Bai* 374

- Effects of Baclofen on Transient Neurons in the Mudpuppy Retina: Electrogenic  
and Network Actions

*S.-H. Bai and M. M. Slaughter* 382

- Encoding of Electrical, Thermal, and Mechanical Noxious Stimuli by Subnucleus  
Reticularis Dorsalis Neurons in the Rat Medulla

*L. Villanueva, Z. Bing, D. Bouhassira, and D. Le Bars* 391

(Continued)

Variance Analysis of Excitatory Postsynaptic Potentials in Cat Spinal Motoneurons During Posttetanic Potentiation <i>H. P. Clamann, J. Mathis, and H.-R. Lüscher</i>	403
Evidence That Repetitive Seizures in the Hippocampus Cause a Lasting Reduction of GABAergic Inhibition <i>J. Kapur, J. L. Stringer, and E. W. Lothman</i>	417
Loss of Inhibition Precedes Delayed Spontaneous Seizures in the Hippocampus After Tetanic Electrical Stimulation <i>J. Kapur and E. W. Lothman</i>	427
Depth Distribution of Neuronal Activity Related to a Visual Reaction Time Task in the Monkey Prefrontal Cortex <i>T. Sawaguchi, M. Matsumura, and K. Kubota</i>	435
Components of the Responses of a Population of DSCT Neurons Determined From Single-Unit Recordings <i>C. E. Osborn and R. E. Poppele</i>	447
Components of Responses of a Population of DSCT Neurons to Muscle Stretch and Contraction <i>C. E. Osborn and R. E. Poppele</i>	456
Announcements	466

#### IMPORTANT CHANGE

As of July 1, 1989, the reference style for the *Journal of Neurophysiology* is changing in text from serial numbering to author's name and date. The unnumbered reference list should continue to be arranged alphabetically by author. See Information for Contributors for details and examples. It will be appreciated if authors of manuscripts submitted under the old system can make these changes during revision.

# JOURNAL OF NEUROPHYSIOLOGY

March 1989  
Volume 61, Number 3

Whole-Cell Patch-Clamp Analysis of Voltage-Dependent Calcium Conductances in Cultured Embryonic Rat Hippocampal Neurons <i>D. E. R. Meyers and J. L. Barker</i>	467
Cytometric Analysis of the Thalamic Ventralis Intermedius Nucleus in Humans <i>T. Hirai, C. Ohye, Y. Nagaseki, and M. Matsumura</i>	478
Further Physiological Observations on the Ventralis Intermedius Neurons in the Human Thalamus <i>C. Ohye, T. Shibasaki, T. Hirai, H. Wada, M. Hirato, and Y. Kawashima</i>	488
Activity-Dependent Disinhibition. I. Repetitive Stimulation Reduces IPSP Driving Force and Conductance in the Hippocampus In Vitro <i>S. M. Thompson and B. H. Gähwiler</i>	501
Activity-Dependent Disinhibition. II. Effects of Extracellular Potassium, Furosemide, and Membrane Potential on $E_{Cl^-}$ in Hippocampal CA3 Neurons <i>S. M. Thompson and B. H. Gähwiler</i>	512
Activity-Dependent Disinhibition. III. Desensitization and GABA <sub>B</sub> Receptor-Mediated Presynaptic Inhibition in the Hippocampus In Vitro <i>S. M. Thompson and B. H. Gähwiler</i>	524
Monkey Primary Motor and Premotor Cortex: Single-Cell Activity Related to Prior Information About Direction and Extent of an Intended Movement <i>A. Riehle and J. Requin</i>	534
Muscle Afferent Contribution to Control of Paw Shakes in Normal Cats <i>A. Prochazka, M. Hulliger, P. Trend, M. Llewellyn, and N. Dürmüller</i>	550
Memory Traces in Primate Spinal Cord Produced by Operant Conditioning of H-Reflex <i>J. R. Wolpaw and C. L. Lee</i>	563
Urinary Bladder and Hindlimb Afferent Input Inhibits Activity of Primate T <sub>2</sub> -T <sub>5</sub> Spinothalamic Tract Neurons <i>T. J. Brennan, U. T. Oh, S. F. Hobbs, D. W. Garrison, and R. D. Foreman</i>	573
Electrophysiological Properties and Synaptic Responses in the Deep Layers of the Human Epileptogenic Neocortex In Vitro <i>M. Avoli and A. Olivier</i>	589
EPSPs in Rat Neocortical Neurons In Vitro. I. Electrophysiological Evidence for Two Distinct EPSPs <i>B. Sutor and J. J. Hablitz</i>	607
EPSPs in Rat Neocortical Neurons In Vitro. II. Involvement of N-Methyl-D-Aspartate Receptors in the Generation of EPSPs <i>B. Sutor and J. J. Hablitz</i>	621

(Continued)

Topographical Distribution and Functional Properties of Cortically Induced Rhythmic Jaw Movements in the Monkey ( <i>Macaca fascicularis</i> ) <i>C.-S. Huang, H. Hiraba, G. M. Murray, and B. J. Sessle</i>	635
Deficits in Reaction Times and Movement Times as Correlates of Hypokinesia in Monkeys With MPTP-Induced Striatal Dopamine Depletion <i>W. Schultz, A. Studer, R. Romo, E. Sundström, G. Jonsson, and E. Scarnati</i>	651
Activity of Hippocampal Formation Neurons in the Monkey Related to a Conditional Spatial Response Task <i>Y. Miyashita, E. T. Rolls, P. M. B. Cahusac, H. Niki, and J. D. Feigenbaum</i>	669
Announcement	679

#### IMPORTANT CHANGE

As of July 1, 1989, the reference style for the *Journal of Neurophysiology* is changing in text from serial numbering to author's name and date. The unnumbered reference list should continue to be arranged alphabetically by author. See Information for Contributors for details and examples. It will be appreciated if authors of manuscripts submitted under the old system can make these changes during revision.

# EPSPs in Rat Neocortical Neurons in Vitro

## II. Involvement of *N*-Methyl-D-Aspartate Receptors in the Generation of EPSPs

BERND SUTOR AND JOHN J. HABLITZ

Section of Neurophysiology, Department of Neurology, Baylor College of Medicine,  
Houston, Texas 77030

### SUMMARY AND CONCLUSIONS

1. Intracellular recordings were obtained from neurons in layer II/III of rat frontal cortex. Single-electrode current- and voltage-clamp techniques were employed to compare the sensitivity of excitatory postsynaptic potentials (EPSPs) and iontophoretically evoked responses to *N*-methyl-D-aspartate (NMDA) to the selective NMDA antagonist D-2-amino-5-phosphonovaleric acid (D-2-APV). The voltage dependence of the amplitudes of the EPSPs before and after pharmacologic changes in the neuron's current-voltage relationship was also examined.

2. NMDA depolarized the membrane potential, increased the neuron's apparent input resistance ( $R_N$ ), and evoked bursts of action potentials. The NMDA-induced membrane current ( $I_{NMDA}$ ) gradually increased with depolarization from -80 to -40 mV. The relationship between  $I_{NMDA}$  and membrane potential displayed a region of negative slope conductance in the potential range between -70 and -40 mV which was sufficient to explain the apparent increase in  $R_N$  and the burst discharges during the NMDA-induced depolarization.

3. Short-latency EPSPs (eEPSPs) were evoked by low-intensity electrical stimulation of cortical layer IV. Changes in the eEPSP waveform following membrane depolarization and hyperpolarization resembled those of NMDA-mediated responses. However, the eEPSP was insensitive to D-2-APV applied at concentrations (up to 20  $\mu$ M) that blocked NMDA responses.

4. EPSPs with latencies between 10 and 40 ms [late EPSPs (lEPSPs)] were evoked by electrical stimulation using intensities just subthreshold to the activation of IPSPs. The amplitude of the lEPSP increased with hyperpolarization and decreased with depolarization.

5. The lidocaine derivative QX-314, injected intracellularly, suppressed sodium-dependent action potentials and depolarizing inward rectification. Simultaneously, the amplitude of the eEPSP significantly decreased with depolarization. Neither the amplitude of a long-latency EPSP nor the amplitude of inhibitory postsynaptic potentials (IPSPs) was significantly affected by QX-314.

6. Cesium ions (0.5–2.0 mM) added to the bathing solution reduced or blocked hyperpolarizing inward rectification. Under these conditions, the amplitude of the eEPSP increased with hyperpolarization. The amplitude of the lEPSP was unaltered or enhanced.

7. The lEPSP was reversibly blocked by D-2-APV (5–20  $\mu$ M), although the voltage-dependence of its amplitude did not resemble the action of NMDA on neocortical neurons. When measured in the same neuron, the amplitude of the membrane current underlying the lEPSP (lEPSC) decreased with depolarization from -80 to -30 mV, whereas in the same potential range, the amplitude of the  $I_{NMDA}$  increased.

8. Induction of long-term potentiation of the lEPSP, observed following high-frequency stimulation (HFS), was suppressed by D-2-APV (10–20  $\mu$ M). Furthermore, this NMDA antagonist was capable of reducing the amplitude of lEPSPs potentiated by HFS.

9. Elevation of extracellular magnesium ( $[Mg^{2+}]_0$ ) from 1.3 to 3.0 mM resulted in a reduction in the amplitude of excitatory and inhibitory postsynaptic potentials. Simultaneously, the response evoked by iontophoretically applied NMDA was decreased. The membrane potential and the  $R_N$  were not affected. Neuronal excitability decreased as indicated by an increase in the rheobase current. A reduction in  $[Mg^{2+}]_0$  led to a depolarization of the membrane potential accompanied by an increase in  $R_N$  and a decrease in rheobase. These changes were insensitive to D-2-APV.

10. Following a decrease in  $[Mg^{2+}]_0$  to nominally 0 mM, spontaneous epileptiform discharges occurred at a rate of 3–7/min. In response to electrical stimulation, the neurons produced all-or-none burst discharges. In the absence of magnesium, graded postsynaptic responses were not obtainable. Spontaneous and evoked bursts induced by removal of  $Mg^{2+}$  ions were reversibly blocked by D-2-APV. The multiple effects produced by alterations in  $[Mg^{2+}]_0$  precluded a simple classification of EPSPs based on their sensitivity to  $Mg^{2+}$  ions.

11. These experiments provide evidence for a D-2-APV-sensitive lEPSP in rat neocortical neurons. Since the electrophysiological properties of the synaptic potential do not agree with an NMDA-mediated postsynaptic mechanism, we propose that the lEPSP is generated by a polysynaptic pathway and that the NMDA receptors responsible for the D-2-APV sensitivity of the lEPSP are located on locally projecting neurons presynaptic to the neuron recorded.

12. In contrast to the lEPSP, NMDA receptors are not involved in the generation of the eEPSP. The parallel changes in the neuron's current-voltage ( $I-V$ ) relationship and in the waveform of the eEPSP recorded at different membrane potentials indicate that the shape of the eEPSP is largely determined by the nonlinear properties of the neuronal membrane.

### INTRODUCTION

Autoradiographic mapping studies in the rat central nervous system have shown that layer II/III of the frontal cortex, together with the CA1 area of the hippocampus and the inner molecular layer of the dentate gyrus, possess the highest density of L-glutamate binding sites sensitive to the excitatory amino acid agonist *N*-methyl-D-aspartate (NMDA) (19). The high density of these presumed NMDA

receptors in the superficial layers of the neocortex suggests that they may be involved in excitatory synaptic transmission mediated by endogenously released excitatory amino acids like L-glutamate or L-aspartate (26). Accordingly, an excitatory postsynaptic potential (EPSP), displaying all the characteristic features of an NMDA-mediated synaptic potential, has been described in the neocortex (32). The amplitude of this EPSP increased with depolarization and decreased with hyperpolarization in a manner similar to the neuron's response to iontophoretically applied NMDA (32, 33). Following a reduction in the extracellular magnesium concentration ( $[Mg^{2+}]_0$ ), a manipulation that relieves NMDA-activated channels from the voltage-dependent, magnesium-induced block (17, 20), the amplitude of the NMDA-mediated EPSP decreased with depolarization and increased with hyperpolarization (32). Furthermore, competitive NMDA antagonists like D-2-amino-5-phosphonovaleric acid (D-2-APV), or noncompetitive NMDA antagonists like ketamine or cyclazocine, were shown to block the NMDA-mediated EPSP in rat neocortical neurons (32, 34, 35).

In the preceding paper (29), we provided evidence for two electrophysiologically distinct EPSPs. Based on a latency criterion, the low-threshold short-latency EPSP was termed the early EPSP (eEPSP), whereas the long-latency EPSP, observed at higher stimulation strengths, was called the late EPSP (lEPSP). The shape of the eEPSP waveform appeared to change following membrane potential shifts in a manner similar to the NMDA-mediated EPSP described previously in rat neocortical neurons (32). However, these changes were not significant and, since other electrophysiological properties were not in agreement with an NMDA-mediated mechanism underlying the eEPSP, we proposed the hypothesis that the eEPSP is generated at synapses remote from the presumed somatic recording site. The shape of the eEPSP detected at this site is therefore determined in large part by the nonlinear properties of the neuronal membrane and by dendritic cable properties (29). On the basis of this hypothesis, three predictions were made: 1) at every membrane potential, the eEPSP should be insensitive to competitive NMDA antagonists (e.g., D-2-APV); 2) changes in the neuron's current-voltage (*I-V*) relationship, induced, for example, by a selective ion-channel blocker, should result in parallel voltage-dependent changes in the eEPSP waveform; and 3) reductions in  $[Mg^{2+}]_0$  should not affect the shape of the eEPSP's waveform. In the present paper, we describe experiments designed to test these predictions and provide evidence for their validity.

In addition to the existence of two different EPSPs, we demonstrated the ability of neocortical neurons to express long-term potentiation (LTP) following tetanic stimulation (29). Furthermore, we showed that high-frequency stimulation (HFS) leading to LTP preferentially affects the lEPSP. Since evidence has been presented that NMDA receptors are involved in the induction of LTP in the CA1 area of the hippocampus (2) and in rat visual cortex (1), we examined the effects of the selective NMDA antagonist D-2-APV on the lEPSP and on the induction of LTP in neurons of the rat frontal cortex. Parts of the material presented has been published in abstract form (27, 28).

## METHODS

The preparation, stimulation, and recording techniques employed were similar to those described in the preceding paper (29). In some experiments, the recording electrodes were filled with a solution of the lidocaine derivative QX-314 (100 mM) in 4 M potassium acetate (KAc), adjusted to pH 7.2 with acetic acid. The diffusion of QX-314 out of the electrode was facilitated by applying cationic current pulses (500 ms, 0.5–1.0 nA) at a frequency of 1 Hz for 30 s to 1 min. We analyzed only those neurons in which the sodium-dependent action potential was found to be irreversibly blocked. When CsCl was added to the bathing solution, an equivalent amount of NaCl was omitted.

The excitatory amino acid agonist NMDA was applied by iontophoresis from one barrel of a double-barreled micropipette using a constant-current device (WPI model 160 microiontophoresis programmers). NMDA (20 mM) was dissolved in a 150-mM sodium phosphate buffer adjusted to pH 8. The second barrel of the micropipette contained 1 M NaCl. The agonist was applied by anionic current that was compensated for by injection of a cationic current of the same magnitude via the NaCl-filled barrel. The micropipette was positioned proximal to the recording electrode and was moved vertically by means of a microdrive. After a stable impalement had been obtained, the iontophoresis electrode was adjusted to achieve a maximal response to NMDA applied by low iontophoresis currents (5–15 nA for 0.5–1.0 s). NMDA was administered in a regular cycle (interval between individual applications at least 60 s). Once a stable response was attained, this cycle was not changed until the end of the experiment. Between applications, a retaining current of 3–5 nA was used to prevent leakage of the agonist out of the pipette. In a few cases, on termination of the recording, NMDA was iontophoresed into the extracellular space using currents similar to those applied during the experiments (maximum, 80 nA), and extracellular DC-potential shifts were determined. As reported previously (8), significant extracellular DC-potential shifts were observed only during application of NMDA using high iontophoretic currents (>120 nA). The NMDA antagonist D-2-APV was added to the bathing solution at concentrations between 5 and 20  $\mu$ M.

When  $Mg^{2+}$  ions were omitted from the bathing solution, they were not substituted for by  $Ca^{2+}$  or other divalent cations. Similarly, enhancements in  $[Mg^{2+}]_0$  were not compensated for by a reduction in the extracellular  $Ca^{2+}$  concentration. Therefore, compared to the normal solution, the total concentration of divalent cations was reduced by 34% in a  $Mg^{2+}$ -free solution and it was increased by 45% when using a solution with 3 mM  $[Mg^{2+}]_0$ . In previous studies (15, 30), atomic absorption spectroscopy measurements of  $Mg^{2+}$  in nominally  $Mg^{2+}$ -free solutions revealed  $Mg^{2+}$  levels of 5–10  $\mu$ M. This residual  $Mg^{2+}$  is due to impurities of the water and the salt compounds used to prepare the bathing solution.

$Mg^{2+}$  ions were typically washed out for 30–60 min after control measurements were performed in the presence of  $Mg^{2+}$ . In some experiments, slices were kept for 1–4 h in a storage chamber containing a  $Mg^{2+}$ -free solution before being transferred to the recording chamber where they were also perfused with  $Mg^{2+}$ -free medium.

## RESULTS

### *Actions of NMDA on rat neocortical neurons*

To allow direct comparisons between the electrophysiological and pharmacological properties of evoked EPSPs and those of NMDA's actions on neocortical neurons, experiments were performed to describe the effects of ionto-

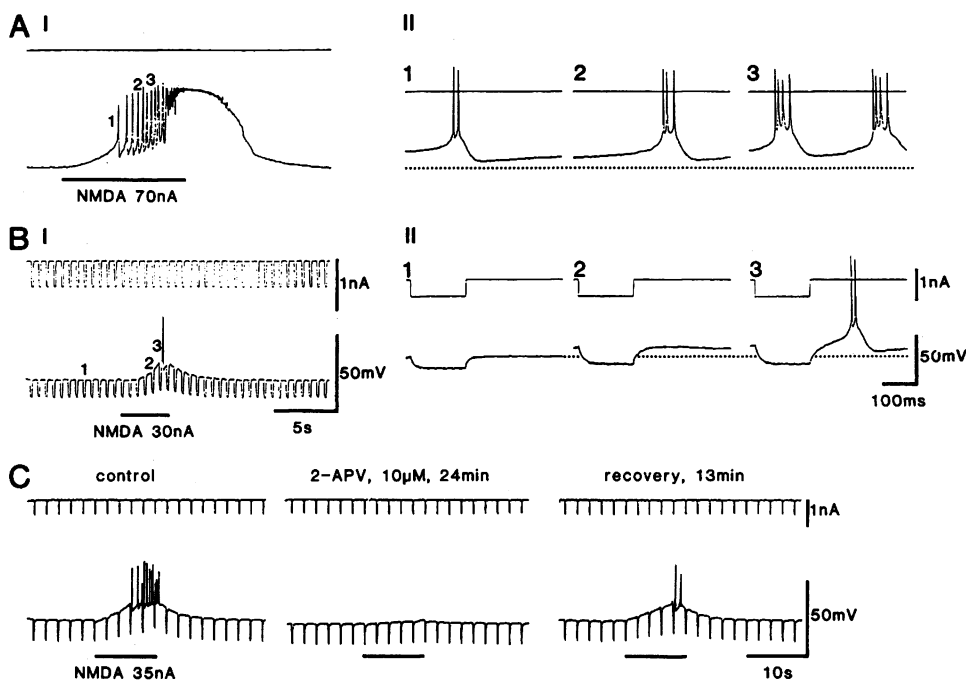


FIG. 1. Responses of neocortical neurons to iontophoretically applied NMDA. *A*, *I*: NMDA administered by iontophoresis with 70 nA for 10 s (indicated by the bar) caused a depolarization of the membrane potential associated with burst discharges. *II*: single bursts (indicated by the numbers 1–3 in part *I*) are depicted on a faster time scale. The neuron's RMP was  $-74$  mV. Calibrations for *A**I* and *A**II* are shown in *B**I* and *B**II*, respectively. In all figures, the upper trace represents the current and the lower trace the voltage. *B*: NMDA-induced depolarization was accompanied by an apparent increase in  $R_N$ . *I*:  $R_N$  was measured by injecting 0.5-nA hyperpolarizing current pulses, 150 ms in duration at a frequency of 2 Hz. *II*: single measurements before and during the application of NMDA (indicated by the numbers 1–3 in part *I*) are presented on a faster time scale. Same cell as in *A*. *C*: D-2-APV ( $10\ \mu M$ ) added to the bathing solution depressed the neuron's response evoked by iontophoretic application of NMDA with 35 nA for 10 s (indicated by the bar). The panel shows chart recordings of NMDA responses before (control), during (D-2-APV,  $10\ \mu M$ , 24 min), and after administration (recovery, 13 min) of D-2-APV. The neuron's RMP was  $-78$  mV.

phoretically applied NMDA on these cells under the present experimental conditions. Typical NMDA-induced responses, quite similar to those reported previously in neocortical neurons (7, 30, 32, 33), are summarized in Fig. 1. After the application of relatively high iontophoretic currents (60–80 nA for 5–15 s) (Fig. 1, *A**I*), NMDA slowly depolarized the membrane potential until a “bursting threshold” was reached [15–25 mV positive to the resting membrane potential (RMP)] (Fig. 1, *A**I*, *I* and *A**II*, *I*). From this potential on, the neuron responded to ongoing NMDA application with characteristic burst discharges followed by afterhyperpolarizations of large amplitude (Fig. 1, *A**I*, *I*–*3* and *A**II*, *I*–*3*). Finally, the amplitude of the afterhyperpolarization gradually declined (Fig. 1, *A**I*), the action potential mechanism inactivated, and the depolarization attained a maximal value (“depolarization block,” Fig. 1, *A**I*). During this plateau phase, the neuronal input resistance ( $R_N$ ) decreased by 75–90%. The recovery from such an extreme NMDA-induced depolarization was complete within 20–30 s. Upon application of NMDA using low iontophoretic currents (20–50 nA for 2–10 s) (Fig. 1, *B**I*), the neuron produced one or several bursts riding on top of a low-amplitude membrane depolarization (Fig. 1, *B**I*, *3* and *B**II*, *3*). The membrane potential reverted to control levels within 5–10 s after the application was terminated.

These response patterns, evoked by NMDA using high and low iontophoretic currents, respectively, were consistent among the neurons tested ( $n = 15$ ).

The NMDA-induced depolarization was associated with an apparent increase in  $R_N$  (Fig. 1, *B**I* and *B**II*). The  $R_N$  was determined by injecting hyperpolarizing current pulses (0.5 nA, 150 ms) and measuring the corresponding voltage deviation before and during the NMDA-induced depolarization (Fig. 1, *B**I*, *I*–*3* and *B**II*, *I*–*3*).

In other neuronal systems, this apparent increase in  $R_N$  has been explained by the characteristic relationship between the NMDA-evoked membrane current ( $I_{NMDA}$ ) and the membrane potential (7, 14, 16). In the potential range from  $-60$  to  $-30$  mV, the  $I_{NMDA}$ -voltage curves displayed a region of negative slope conductance that accounted for the apparent increase in  $R_N$  during NMDA-evoked depolarizations (7, 15, 17). To test the validity of this hypothesis in rat neocortical neurons, measurements of the NMDA-induced currents at different holding potentials were performed using the single-electrode voltage-clamp technique. Our observations (presented in Fig. 8) suggest that the mechanisms leading to the apparent increase in  $R_N$  during the NMDA-evoked depolarization in rat neocortical neurons are identical to those described in other types of neurons (7, 15, 17) (for review see Ref. 16).

All NMDA-induced effects described thus far were reversibly blocked when the NMDA antagonist D-2-APV was added to the bathing solution at concentrations between 5 and 20  $\mu\text{M}$ . Figure 1C depicts the effect of D-2-APV on NMDA-induced depolarization, bursting, and resistance increase. In this and all other neurons tested ( $n = 17$ ), D-2-APV had no detectable effect on RMP,  $R_N$ , or the generation of action potentials induced by depolarizing current pulses.

#### Sensitivity of the eEPSP to D-2-APV

eEPSPs were evoked by electrical stimulation of cortical layer IV using stimulation intensities between 0.1 and 0.35 T (where T is the threshold intensity required to elicit an action potential at RMP) (see Fig. 2, control, -72 mV). As described in the preceding paper (29), the amplitude of the eEPSP decreased with hyperpolarization and increased insignificantly with depolarization to subthreshold levels (Fig. 2, control, -57 mV). This voltage dependence of the EPSP amplitude resembled the changes in the amplitudes of NMDA-induced depolarizations following shifts of the membrane potential in hyperpolarizing and depolarizing directions, respectively (not shown). However, when D-2-APV was added to the bathing solution (Fig. 2, D-2-APV, 10  $\mu\text{M}$ ) at concentrations that completely blocked or significantly reduced the response produced by iontophoretically applied NMDA (see Figs. 1C and 7B), the amplitude of the eEPSP was unaltered (Fig. 2, compare eEPSPs at -72 mV). In 6 neurons, the mean amplitude of the eEPSP, measured at RMP, was  $5.8 \pm 2.6$  (SD) mV under control conditions and  $6.2 \pm 2.3$  mV after addition of D-2-APV to the bathing solution. When the membrane potential was depolarized to subthreshold levels, the associated changes in the shape of the eEPSP were unaffected by D-2-APV (Fig. 2, compare eEPSPs at -57 mV). After depolarization to the threshold potential (Fig. 2, control, -53 mV), D-2-APV influenced neither the threshold level nor the form of action potential discharge elicited by the eEPSP (Fig. 2, compare eEPSPs at -53 mV).

#### Sensitivity of the eEPSP to QX-314 and cesium ions

In the preceding paper (29), we proposed that the shape of the eEPSP at different membrane potentials is partly

determined by the nonlinear properties of the neuronal membrane (see also Ref. 24). To test this hypothesis, substances known to change the neuron's  $I$ - $V$  relationship were applied. In a first set of experiments, QX-314 was injected into neurons via the recording electrode. This lidocaine derivative blocks the sodium conductance underlying the action potential and inhibits a slowly inactivating or noninactivating, tetrodotoxin-sensitive sodium conductance (3, 4, 24) that is, in part, responsible for the inward rectification in the depolarizing direction observed in neocortical neurons (3, 24, 25, 31).

Approximately 5–10 min after impalement of a neuron with an electrode containing 100 mM QX-314, the fast action potential was irreversibly blocked, and the  $R_N$ , determined at RMP by injecting small hyperpolarizing current pulses, was increased by 10–20%. The RMP did not differ significantly from that of normal neurons. After depolarization of the membrane potential by 35–45 mV using current pulses 150–200 ms in duration, slow, all-or-none events were observed (Fig. 3A) which were similar to calcium-dependent action potentials reported previously in this preparation (31). As soon as the sodium action potentials were blocked and slow spikes could be evoked by depolarizing current injection (Fig. 3A), depolarizing inward rectification was virtually absent in these neurons. Figure 3B shows the determination of  $R_N$  at different membrane potentials using small hyperpolarizing current pulses. The measurements were performed 2 min after the records depicted in Fig. 3A were made. From the amplitude of the voltage deviation produced by the inward current pulse,  $R_N$  was calculated and plotted as a function of the membrane potential (Fig. 3C). The diagram clearly shows that the  $R_N$  decreased with hyperpolarization (Fig. 3C, squares); but with regard to the RMP (-79 mV), the  $R_N$  did not change significantly upon depolarization. For comparison, the relationship between  $R_N$  and RMP is shown in a control neuron impaled with a KAc-filled electrode (Fig. 3C, circles). The rectification ratio, calculated from the quotient of the  $R_N$  at -55 mV and at -80 mV (29), ranged between 0.8 and 1.1 in QX-314-injected neurons ( $n = 5$ ) and was  $1.77 \pm 0.39$  (SD) in neurons recorded with a KAc-filled electrode ( $n = 15$ ). These results are in agreement with previous studies in which QX-314 effectively blocked the depolarizing inward rectification in neocortical neurons (3, 24). In addition, we found that QX-314 did not alter the hyperpolarizing inward rectification (Fig. 3, B and C).

According to our hypothesis (see Ref. 29), the QX-314-induced changes in the  $I$ - $V$  relationship should be associated with a change in the voltage-dependence of the eEPSP amplitude recorded at the soma. In fact, in all neurons tested ( $n = 5$ ), we observed a decrease in the eEPSP amplitude with depolarization and a slight increase or no change in amplitude with hyperpolarization. Figure 4 shows the behavior of the eEPSP amplitude following changes in membrane potential in QX-314 injected cells compared with an eEPSP recorded in neurons impaled with KAc-filled electrodes. In the neurons depicted in Fig. 4, A and B, the membrane potential was changed by injection of DC pulses 1 s in duration. Between the individual current injections, recordings were made of the eEPSP at

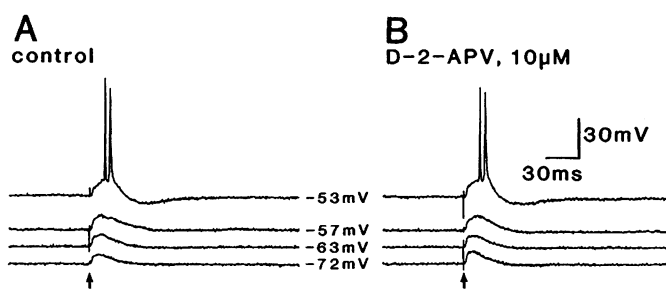


FIG. 2. Insensitivity of the eEPSP to D-2-APV. A: in the absence of D-2-APV, an eEPSP was evoked by electrical stimulation with 10 nC (0.17 T) at different membrane potentials (in all figures, stimulation is indicated by arrows). The membrane potential was displaced by current pulses of 1-s duration at a frequency of 0.1 Hz. B: D-2-APV (10  $\mu\text{M}$ ) was added to the bathing solution, and the measurements were repeated 15 min after onset of application. The neuron's RMP was -72 mV.

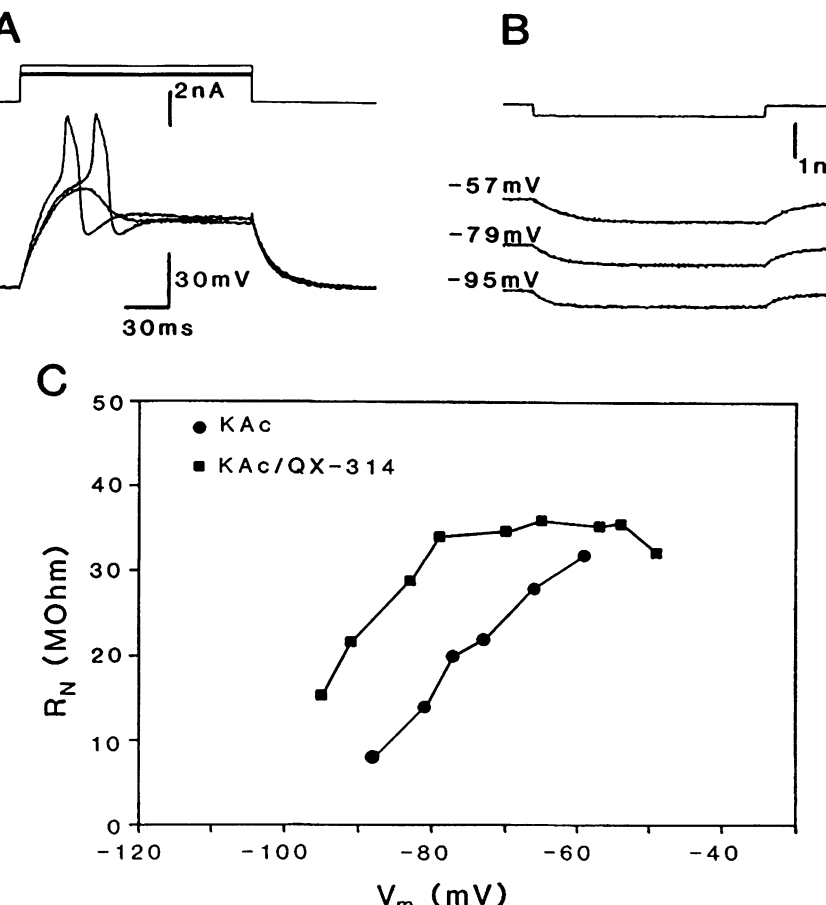


FIG. 3. Electrophysiological properties of neurons injected with QX-314. *A*: after injection of QX-314 (500-ms depolarizing current pulses, 0.7 nA at 1 Hz for 45 s), the neuron responded to outward current pulses, using threshold (1.6 nA) and suprathreshold (2.0 nA) intensities, with slow, all-or-none spike potentials. Just subthreshold current pulses evoked a transient depolarizing potential. The neuron's RMP was -79 mV. *B*: determination of  $R_N$  at different membrane potentials by injecting hyperpolarizing current pulses (0.4 nA, 150 ms) and measuring the corresponding voltage deviation just before the offset of the pulse. Same neuron as in *A*. *C*: plot of  $R_N$  as a function of membrane potential in a neuron injected with QX-314 (squares; same cell as in *A* and *B*). For comparison, the relationship between  $R_N$  and membrane potential is shown in a normal neuron (RMP, -81 mV; circles).

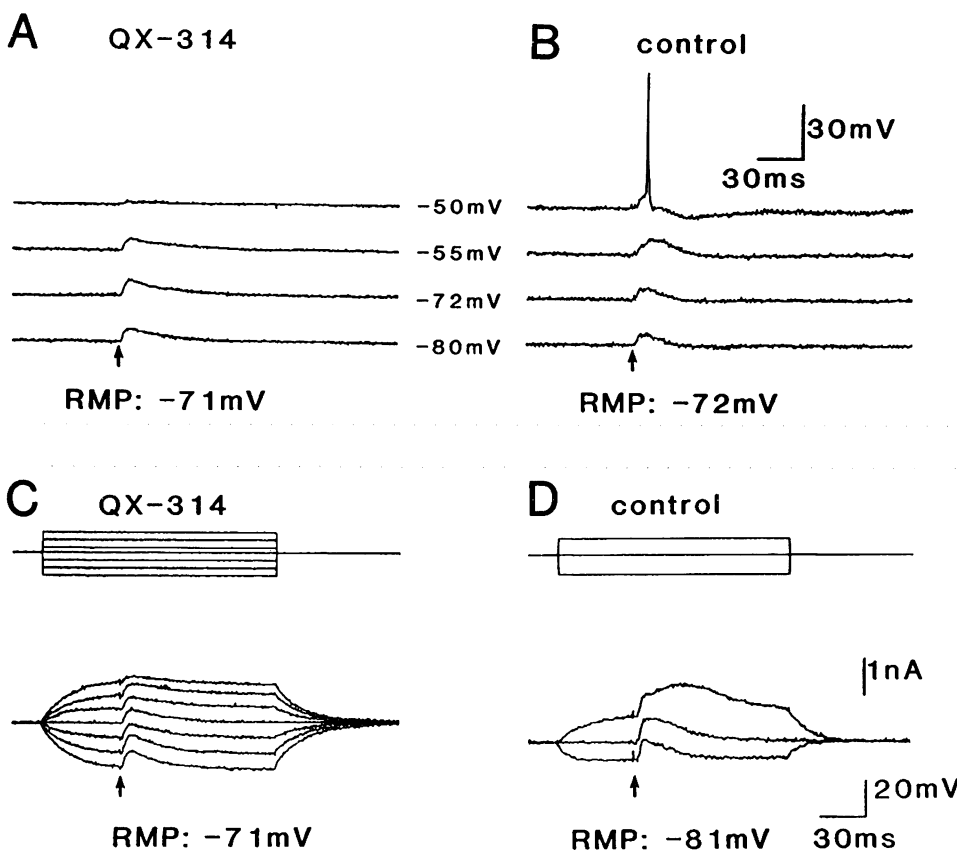


FIG. 4. Influence of QX-314 on the shape of the eEPSP waveform at different membrane potentials. *A*: eEPSPs were evoked by electrical stimulation with 6 nC (0.19 T) at different membrane potentials. QX-314 was injected into the neuron using 500-ms depolarizing current pulses of 0.6 nA at a frequency of 1 Hz for 1 min (RMP, -72 mV). The membrane potential was displaced by direct current pulses 1 s in duration. *B*: relationship between eEPSP waveform and membrane potential in a neuron recorded with a KAc electrode (stimulus intensity, 8 nC = 0.21 T; RMP, -74 mV). *C*: another example of the behavior of the eEPSP in a QX-314-injected neuron. Stimulus intensity, 8 nC = 0.29 T; RMP, -71 mV. The membrane potential was shifted by depolarizing and hyperpolarizing current pulses 150 ms in duration. *D*: different neuron recorded with a KAc-filled electrode. RMP, -81 mV.

control levels to check for any alterations. In the other neurons (Fig. 4, C and D), the membrane potential was shifted by shorter current pulses. At RMP, the amplitudes of the eEPSPs evoked in QX-314-injected neurons were not significantly different from those of eEPSPs in normal neurons (Fig. 4, A and B, traces at -72 mV). However, upon depolarization of injected cells, the amplitudes of the eEPSPs decreased considerably (Fig. 4, A and C), and at membrane potentials near or positive to -50 mV, the eEPSPs virtually disappeared. In no case was an increase in the eEPSP amplitude, duration, or time to peak observed in QX-314-injected neurons. QX-314 had no significant effect on the voltage dependence of the IEPSP or that of the chloride- or potassium-dependent IPSPs (evoked at higher stimulus strengths). These findings suggest a correlation between changes in the neuron's *I-V* relationship and the shape of the eEPSP waveform.

In a second series of experiments, cesium was added to the bathing solution. Extracellularly applied cesium ions

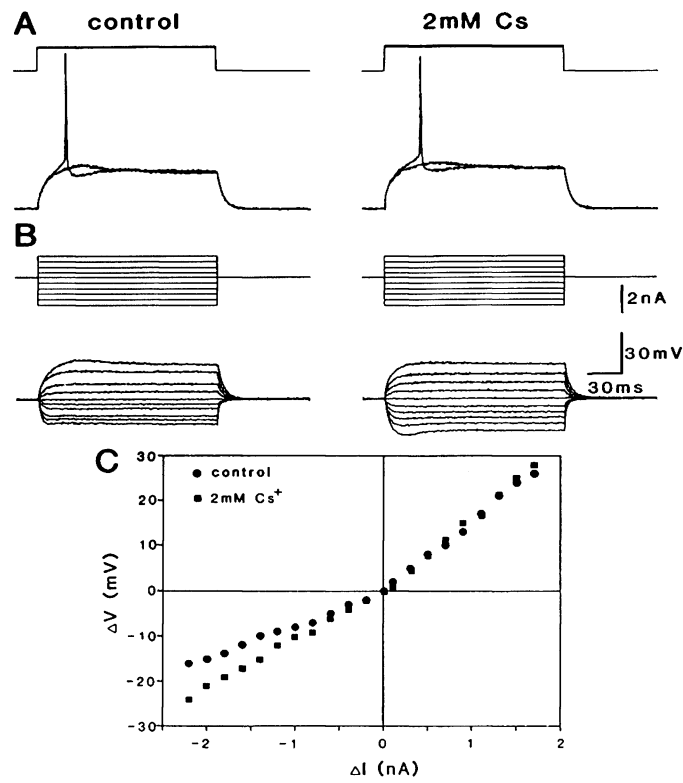


FIG. 5. Effects of cesium ions on the *I-V* relationship in neocortical neurons. A: subthreshold and threshold responses induced by depolarizing current pulses without (control) and with 2 mM CsCl in the bathing solution (10 min). Under control conditions, the neuron's RMP was -82 mV. Upon application of 2 mM CsCl, the membrane potential depolarized to -76 mV. For comparison, the membrane potential was set back to -82 mV by injection of hyperpolarizing current. Without Cs, the current strength necessary to evoke an action potential was 1.8 nA; with Cs, it was 1.9 nA. B: determination of an *I-V* curve without (control) and with 2 mM CsCl in the bathing solution. Depolarizing and hyperpolarizing currents were injected, and the amplitude of the corresponding voltage deviation was measured just before offset of the current pulse. Same cell as in A. When Cs was present, the membrane potential was held at -82 mV by hyperpolarizing current injection. C: plot of the voltage change as a function of the amplitude of the corresponding current pulse (*I-V* curve). The circles represent the *I-V* curve in the absence of Cs, the squares in its presence (same cell in A and B).

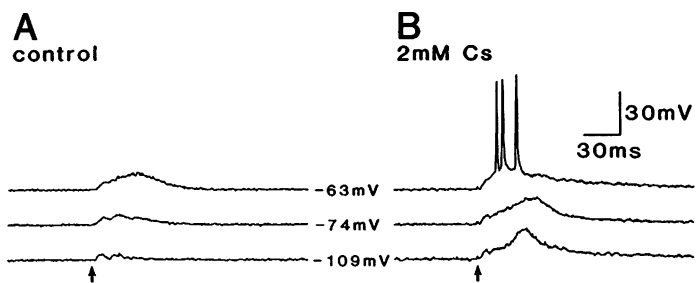


FIG. 6. Influence of cesium ions on eEPSPs and IEPSPs in neocortical neurons. A: in this neuron (RMP, -74 mV), electrical stimulation with an intensity of 7.5 nC (0.32 T) evoked a composite EPSP consisting of an eEPSP and an IEPSP (control, -74 mV). Upon hyperpolarization (1-s pulse), the amplitude decreased (control, -109 mV), and on depolarization, it increased (control, -63 mV). B: after addition of 2 mM CsCl to the bathing solution (12 min), the membrane potential depolarized to -67 mV, and a stimulus with an intensity of 7.5 nC produced a large IEPSP, the amplitude of which increased slightly with hyperpolarization. Cs simultaneously blocked the hyperpolarizing inward rectification in this neuron.

are capable of reducing or blocking inward rectification in hyperpolarizing direction (5, 6, 10, 13, 14, 23). By measuring *I-V* curves in the absence (Fig. 5B, left, and 5C, circles) and presence (Fig. 5B, right, and 5C, squares) of 0.5–2.0 mM cesium, we were able to verify this observation. In the neuron depicted in Fig. 5, 2 mM cesium suppressed the hyperpolarizing inward rectification without affecting the *I-V* curve determined in the depolarizing direction (Fig. 5C). Furthermore, neither the action potential threshold nor the shape of the spike was significantly influenced by cesium (Fig. 5A, control and 2 mM Cs).

In the presence of cesium, the amplitude of the eEPSP increased with hyperpolarization in all neurons tested ( $n = 7$ ). In addition, alterations in synaptic efficacy were observed, as shown in Fig. 6. In this neuron, a stimulus intensity was chosen which evoked an eEPSP followed by a small IEPSP (Fig. 6, control, -74 mV). In the absence of cesium (Fig. 6, control), the amplitude of this composite EPSP increased when the membrane potential was depolarized from the resting level of -74 to -63 mV and decreased with hyperpolarization. In the presence of 2 mM cesium, however, the synaptic response to the same stimulus was completely changed. At a membrane potential of -74 mV, the stimulus evoked an eEPSP followed by a well-expressed IEPSP (Fig. 6, right, 2 mM Cs). The amplitude of this IEPSP increased with hyperpolarization and reached threshold levels upon depolarization (Fig. 6, right, 2 mM Cs), suggesting that, under normal conditions, the conductance underlying the hyperpolarizing inward rectification is strong enough at membrane potentials negative to the RMP to shunt the amplitudes of eEPSPs and weakly expressed IEPSPs. These experiments provide further evidence that voltage-dependent conductances are able to shape the waveform of EPSPs recorded in rat neocortical neurons.

#### Sensitivity of the IEPSP to D-2-APV

In contrast to the eEPSP, the IEPSP evoked by stimulation with intensities between 0.4 and 0.5 T was completely and reversibly blocked by D-2-APV. When tested in the

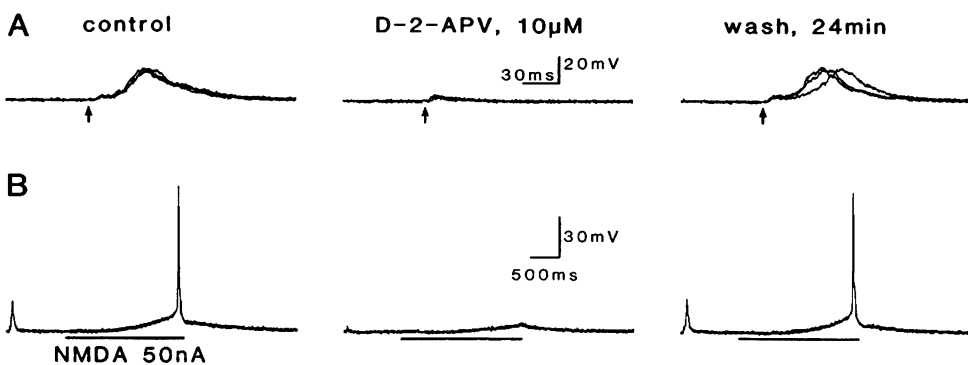


FIG. 7. Block of the IEPSP and the neuron's response to iontophoretically applied NMDA by D-2-APV. *A*: IEPSPs were evoked by electrical stimulation with an intensity of 8 nC (0.35 T) before (control), during (D-2-APV, 10  $\mu$ M), and following (wash, 24 min) administration of D-2-APV. D-2-APV was added to the bathing solution, and measurements were taken 6 min after the start of application. Each panel shows 3 consecutively performed recordings superimposed (RMP, -85 mV). *B*: block of NMDA-induced responses in the same cell. One second after the stimulus, NMDA was applied by iontophoresis (50 nA for 2 s, as indicated by the bar) before (control), during (D-2-APV, 10  $\mu$ M), and after (wash, 24 min) administration of D-2-APV. The voltage deflection at the beginning of each trace represents the stimulus-evoked IEPSP shown in *A*.

same neuron (Fig. 7), the concentration of D-2-APV necessary to suppress the IEPSP was high enough to significantly reduce or block a simultaneously recorded response to iontophoretically applied NMDA. In the experiment shown in Fig. 7, electrical stimulation evoked a small eEPSP followed by an IEPSP (Fig. 7*A*, control). Approximately 1 s after the synaptic response, NMDA was applied by iontophoresis using currents that elicited one burst discharge on top of a slow depolarization (Fig. 7*B*, control). Both the synaptic response produced by electrical stimulation and the response to iontophoretically applied NMDA were blocked after the addition of 10  $\mu$ M D-2-APV to the bathing solution (Fig. 7, *A* and *B*, center traces). Upon removal of D-2-APV from the medium, both responses recovered to control levels (Fig. 7, *A* and *B*, right traces).

The inhibition of the IEPSP by D-2-APV was an unexpected finding, since the amplitude of both the IEPSP and IEPSC increased with hyperpolarization and decreased with depolarization (29). Furthermore, when compared in the same neuron, the voltage dependence of the IEPSC amplitude and that of the  $I_{\text{NMDA}}$  were different ( $n = 4$ , Fig. 8). Figure 8*A* shows an example of such a measurement. The membrane potential was voltage-clamped to different holding potentials ( $V_H$ ), and NMDA was applied by iontophoresis for 1 s. In the potential range investigated (-100 to -40 mV), the  $I_{\text{NMDA}}$  increased with depolarization (Fig. 8*A*). The plot of peak amplitude of  $I_{\text{NMDA}}$  as a function of  $V_H$  (Fig. 8*D*, circles) resulted in an  $I_{\text{NMDA}}$ -voltage relationship with a negative slope conductance in the potential range between -70 and -40 mV. Similar results were obtained in seven neurons.  $I_{\text{NMDA}}$  gradually increased with depolarization from -80 to -40 mV (Fig. 8*A*), yielding an  $I$ - $V$  curve with a region of negative slope conductance (Fig. 8*D*). However, in the same neuron, the simultaneously measured IEPSC decreased slightly with depolarization of the membrane potential from -80 to -40 mV (Fig. 8, *B* and *D*). In the neuron depicted in Fig. 8, the IEPSP elicited by electrical stimulation was preceded by a low-amplitude eEPSP (Fig. 8*C*). The two peaks of the synaptic current recorded at a  $V_H$  of -80 mV (Fig. 8*B*, left trace) correspond

to the eEPSP and the IEPSP, respectively. Upon depolarizing  $V_H$ , a slight decrease in the amplitude of the second peak, representing the IEPSC, was observed (Fig. 8*B*, center and right traces). This finding indicates that the NMDA receptors responsible for the D-2-APV sensitivity of the IEPSP were not located on the neuron recorded, suggesting that a polysynaptic pathway was involved in the generation of the IEPSP.

We demonstrated that HFS led to a sustained increase in the amplitude of the IEPSP (LTP) (29). Because the induction of LTP in hippocampal CA1 neurons (2) and in neurons of the rat visual cortex (1) was blocked by D-2-APV, we investigated the influence of the NMDA antagonist on the expression of LTP in neocortical neurons. An example of such an experiment is shown in Fig. 9*A*. An IEPSP was evoked by electrical stimulation using an intensity of 9 nC (0.36 T) at a stimulus frequency of 0.1 Hz (Fig. 9*A*, first trace). After a control period of 30 min, 20  $\mu$ M D-2-APV was added to the bathing solution; after 4 min, the IEPSP was suppressed (Fig. 9*A*, second trace). HFS was performed 6 min later in the presence of D-2-APV; 2 min after HFS, the antagonist was then washed out. Even after a wash period of 60 min, the amplitude of the IEPSP was not potentiated (Fig. 9*A*, fourth trace) compared with control (Fig. 9*A*, first trace). After complete washout of D-2-APV, LTP could be induced in the same neuron using the same stimulus pattern as in the presence of D-2-APV. Similar results were obtained in three neurons.

In contrast to hippocampal neurons, D-2-APV in neocortical neurons suppressed the amplitudes of IEPSPs potentiated by HFS as well as blocking induction of LTP. In the neuron shown in Fig. 9*B*, the amplitude of the IEPSP evoked by stimulation using a stimulus strength subthreshold for the IEPSP (Fig. 9*B*, control) was considerably potentiated by HFS and attained a constant (suprathreshold) level within 34 min after the tetanus (Fig. 9*B*, second trace). The application of 20  $\mu$ M D-2-APV for 2 min led to a drastic reduction in IEPSP amplitude (Fig. 9*B*, third trace). After washout of D-2-APV, the reduction in IEPSP amplitude was completely reversible (Fig. 9*B*, fourth trace).

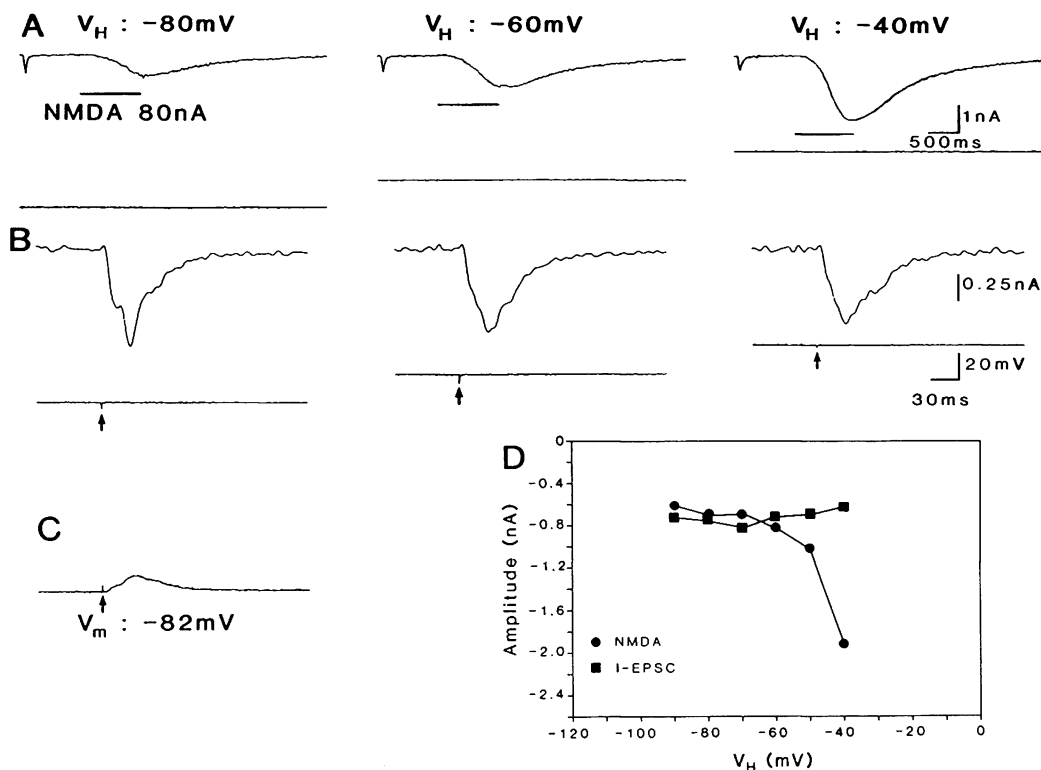


FIG. 8. Comparison of the voltage dependence of the IEPSC and  $I_{NMDA}$  in the same neocortical neuron. *A*: measurements of membrane currents induced by iontophoretically applied NMDA (80 nA for 1 s, as indicated by the bar) at different holding potentials ( $V_H$ ). Each trace represents the average of 3 single measurements. Voltage calibration in *A* is the same as in *B*. *B*: voltage-clamp recordings of synaptic currents evoked by electrical stimulation with an intensity of 19 nC (0.45 T) at different holding potentials ( $V_H$ ). Each trace represents the average of 5 single measurements. *C*: synaptic potential recorded at RMP (-82 mV) in response to a stimulus with an intensity of 19 nC. *D*: plot of IEPSC and  $I_{NMDA}$  peak amplitudes as a function of  $V_H$ .

#### Effects of alterations in $[Mg^{2+}]_0$

Alterations in  $[Mg^{2+}]_0$  significantly affected the intrinsic membrane properties of neocortical neurons. Following a

decrease in  $[Mg^{2+}]_0$ , an increase in the neurons' direct excitability was observed in all neurons tested ( $n = 5$ ). As shown in Fig. 10*A*, the rheobase current (i.e., threshold current intensity necessary to evoke one action potential)

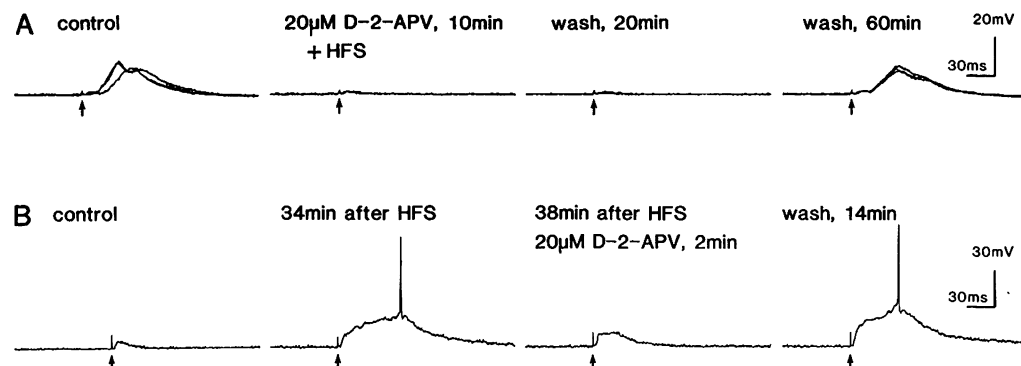


FIG. 9. D-2-APV blocks the induction of LTP and reduces the amplitude of potentiated IEPSPs. *A*: synaptic responses of a neuron (RMP, -79 mV) to stimulation with 9 nC (0.37 T) at a frequency of 0.1 Hz. Control traces represent 3 superimposed averages of 10 consecutive recordings taken 10, 4, and 2 min before application of D-2-APV. After the block of the IEPSP by D-2-APV, HFS (4 trains of 100 Hz for 1 s at 5-s intervals) was performed in the presence of D-2-APV (20  $\mu$ M, 10 min, 2 superimposed averages of 10 single recordings taken 4 and 10 min after application of D-2-APV). D-2-APV washout was begun 2 min after HFS, and after a wash period of 30–60 min, the IEPSP had recovered, but was not enhanced, compared with control (wash, 60 min; 3 superimposed averages of 10 single recordings made 35, 40, and 60 min after HFS). *B*: in another neuron (RMP, -76 mV), a single 22.5-nC stimulus (0.31 T) evoked an eEPSP before HFS (control), and an eEPSP accompanied by a superimposed IEPSP 34 min after HFS (1 train of 100 Hz for 1 s at one-half eEPSP threshold). Note the generation of an action potential by the IEPSP. This enhanced IEPSP was reversibly reduced by the addition of 20  $\mu$ M D-2-APV to the bathing solution.

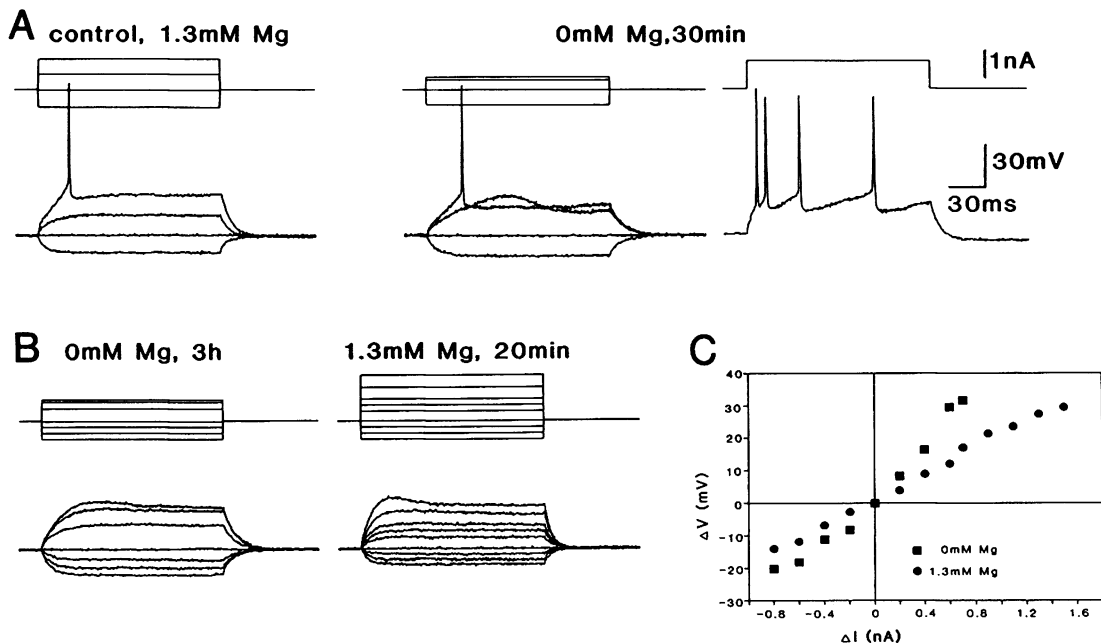


FIG. 10. Effects of alterations in  $[Mg^{2+}]_0$  on membrane properties. *A*: responses to current pulses before and after lowering  $[Mg^{2+}]_0$ . Leftmost panel shows response to a hyperpolarizing current pulse of 0.6 nA and depolarizing pulses of 0.6 and 1.1 nA. Middle panel presents response to a 0.5-nA hyperpolarizing pulse and 0.5- and 0.6-nA depolarizing pulses, indicating an increase in resistance and decrease in threshold. The rightmost panel shows repetitive firing evoked by a 1.1-nA depolarizing current pulse. The neuron had depolarized by 5 mV in the absence of  $Mg^{2+}$  and was returned to the initial RMP ( $-78$  mV) by passing steady current. *B*: specimen records obtained in another neuron in the absence (leftmost traces) and presence (rightmost traces) of 1.3 mM  $[Mg^{2+}]_0$ . *C*:  $I$ - $V$  curve from neuron shown in *B*. RMP in 1.3 mM  $Mg^{2+}$ ,  $-86$  mV.

decreased in the absence of magnesium. The rheobase current was found to be decreased by 0.5–0.8 nA (control values: 1.0–1.5 nA). Furthermore, the frequency of action potential discharge evoked by suprathreshold depolarizing current pulses increased after removal of magnesium (Fig. 10*A*, rightmost trace). These effects were reversible upon returning to normal  $[Mg^{2+}]_0$ . In addition to these effects, a decrease in  $[Mg^{2+}]_0$  to nominally 0 mM led to a depolarization of the membrane potential by 3–5 mV, associated with an increase in  $R_N$  by 20–40%. These observations were consistent among all the neurons tested ( $n = 6$ ).

Determination of  $I$ - $V$  curves in the absence and presence of  $Mg^{2+}$  ions (Fig. 10, *B* and *C*) ( $n = 2$ ) revealed an increase in the slope of the curve. This rise in slope resistance was most pronounced during the injection of depolarizing current pulses (Fig. 10*C*). The consequence of this enhancement in depolarizing inward rectification was an increase in the neuron's direct excitability following removal of  $Mg^{2+}$  ions from the bathing medium.

Elevation of  $[Mg^{2+}]_0$  from 1.3 to 3.0 mM produced a general depression of excitatory and inhibitory synaptic transmission in all neurons tested ( $n = 5$ ). Following an increase in  $[Mg^{2+}]_0$ , the amplitudes of EPSPs and IPSPs were found to be decreased by 40–50% (Fig. 11*A*). A decrease in a depolarizing IPSP is indicated by the results with the 90 nC stimulus. Prior to elevation of  $Mg^{2+}$ , no IEPSP is seen due to a shunting effect of an IPSP. When this IPSP is decreased in elevated  $Mg^{2+}$ , there is an apparent increase in the IEPSP. A selective depression of the D-2-APV-sensitive IEPSP was never observed. Measure-

ments of the reversal potential of the chloride-dependent IPSP ( $E_{IPSP}$ ) in two neurons revealed no changes in  $E_{IPSP}$  (1.3 mM  $[Mg^{2+}]_0$ :  $E_{IPSP} = -67$  and  $-70$  mV; 3.0 mM  $[Mg^{2+}]_0$ :  $E_{IPSP} = -67$  and  $-71$  mV), although, at 3 mM  $[Mg^{2+}]_0$ , the amplitude was decreased. The reduction in the amplitude of the postsynaptic potentials therefore appears due to a decrease in the synaptic conductance rather than a shift in the corresponding reversal potentials.

In agreement with a previous investigation in neocortical neurons (30), a reduction in  $[Mg^{2+}]_0$  to nominally 0 mM led to the development of spontaneous and evoked epileptiform discharges in all neurons tested ( $n = 5$ ). Graded EPSPs or IPSPs were not obtainable after removal of magnesium. Figure 12 depicts postsynaptic responses in the presence and absence of  $Mg^{2+}$  ions. Stimulation at an intensity of 15 nC elicited a composite EPSP consisting of an eEPSP and a IEPSP (Fig. 12*B*, left). Two minutes after removal of  $Mg^{2+}$  ions, the amplitude of the composite EPSP was increased by  $\sim 100\%$  (Fig. 12*B*, center). Four minutes after magnesium removal, the synaptic response was further enhanced and evoked action potentials (Fig. 12*B*, right). In order to detect graded postsynaptic potentials in the absence of  $Mg^{2+}$  ions, stimulus strengths well below the threshold for the elicitation of eEPSPs in the presence of  $Mg^{2+}$  ions were also tested. As shown in Figure 12*A* (left), a 6-nC stimulus initially evoked no response. The threshold intensity for the eEPSP was 12 nC. Seven minutes following the removal of  $Mg^{2+}$  ions from the bathing solution, the 6-nC stimulus evoked an all-or-nothing response which produced action potentials (Fig. 12*A*,

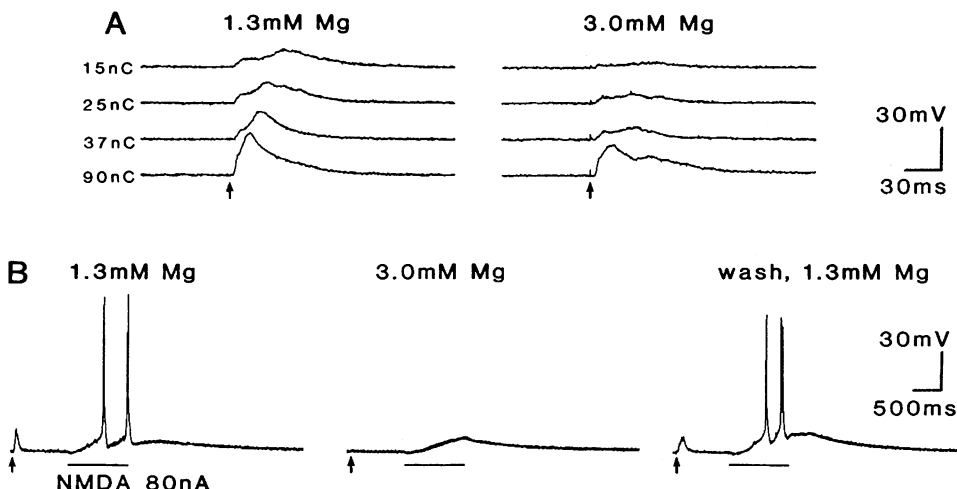


FIG. 11. Changes in postsynaptic potentials and in depolarizations induced by iontophoretically applied NMDA following an increase in [Mg<sup>2+</sup>]<sub>0</sub> to 3 mM. *A*: postsynaptic potentials recorded in response to stimulation with increasing intensity in presence of 1.3 (left) and 3.0 mM [Mg<sup>2+</sup>]<sub>0</sub> (right). The stimulus strengths are given at the left panel. The recordings depicted in the right panel were taken 10 min after changing [Mg<sup>2+</sup>]<sub>0</sub> in the bathing solution. (RMP = -84 mV). Note the decrease in the amplitudes of all postsynaptic potentials. The presence of an IPSP evoked by a stimulus with an intensity of 90 nC (left panel) was verified by reversing the polarity of the potential upon depolarization of the membrane potential. *B*: responses of the same neuron to iontophoretically applied NMDA (80 nA for 1 s) in the presence of a [Mg<sup>2+</sup>]<sub>0</sub> of 1.3 (left) and 3.0 mM, respectively (center). The right panel demonstrates the reversibility of the effect 25 min following the reduction in the [Mg<sup>2+</sup>]<sub>0</sub> from 3.0 to 1.3 mM. The arrow at the beginning of each trace indicates the response of the neuron to a stimulus with an intensity of 25 nC.

center). The latencies of these responses ranged between 50 and 150 ms. After 30 min without Mg<sup>2+</sup> ions, the 6-nC stimulus elicited an all-or-nothing burst discharge (Fig. 12A, right). Stimulus strengths < 6 nC were ineffective.

The all-or-nothing characteristics of the burst discharges occurring in the absence of Mg<sup>2+</sup> ions is demonstrated in more detail in Fig. 13. The recordings shown in this figure were taken from a neuron in a slice which was kept in a Mg<sup>2+</sup>-free solution for >4 h. The stimulus strength necessary to evoke a burst discharge was termed burst threshold

T (Fig. 13A). A 0.75-T stimulus was not able to produce a detectable postsynaptic response (Fig. 13A), whereas a 10-fold increase in the stimulus strength did not enhance the amplitude or pattern of the burst discharge (Fig. 13A).

The burst discharges induced by removal of Mg<sup>2+</sup> ions from the bathing solution occurred either in response to an electrical stimulus (Fig. 13A) or spontaneously at a rate of 3–7 bursts per minute (Fig. 13B). These bursts appear to be generated by synaptic mechanisms, since hyperpolarization and depolarization of the membrane potential resulted

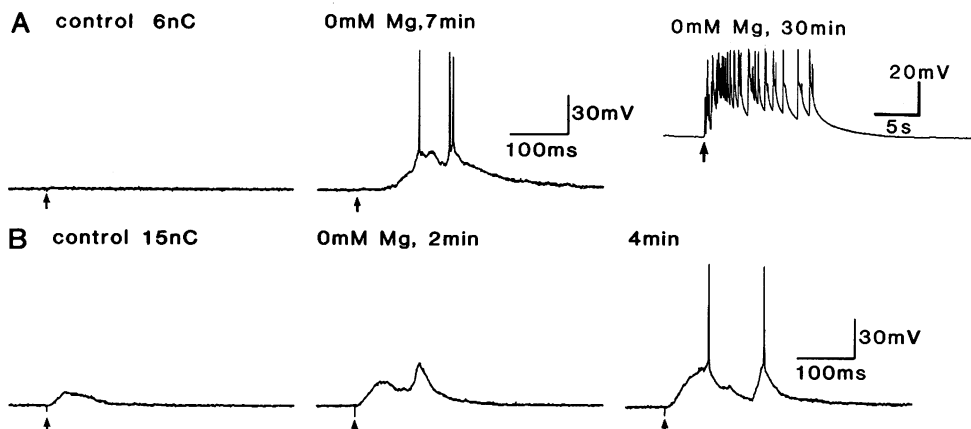


FIG. 12. Development of epileptiform burst discharges following a reduction in [Mg<sup>2+</sup>]<sub>0</sub> to nominally 0 mM. *A*: at normal [Mg<sup>2+</sup>]<sub>0</sub> a stimulus intensity (6 nC) below the threshold for elicitation of an eEPSP was applied (left, threshold intensity was 12 nC). Seven minutes following a decrease in [Mg<sup>2+</sup>]<sub>0</sub> to 0 mM, this stimulus intensity produced, at a latency of 55 ms, an all-or-nothing, suprathreshold burst response (center), and, after 30 min, an all-or-nothing epileptiform burst discharge (right, chart writer recording, action potentials are truncated). Note the difference in the time scale. The membrane potential of the neuron depolarized by 5 mV upon removing Mg<sup>2+</sup> ions. *B*: under control conditions (left) a stimulus with an intensity of 15 nC evoked a composite EPSP (RMP = -78 mV). Two minutes after the removal of Mg<sup>2+</sup> ions, the same stimulus produced an enhanced response (center). After 4 min, the stimulus-evoked suprathreshold postsynaptic potentials (right). Same neuron as in *A*.

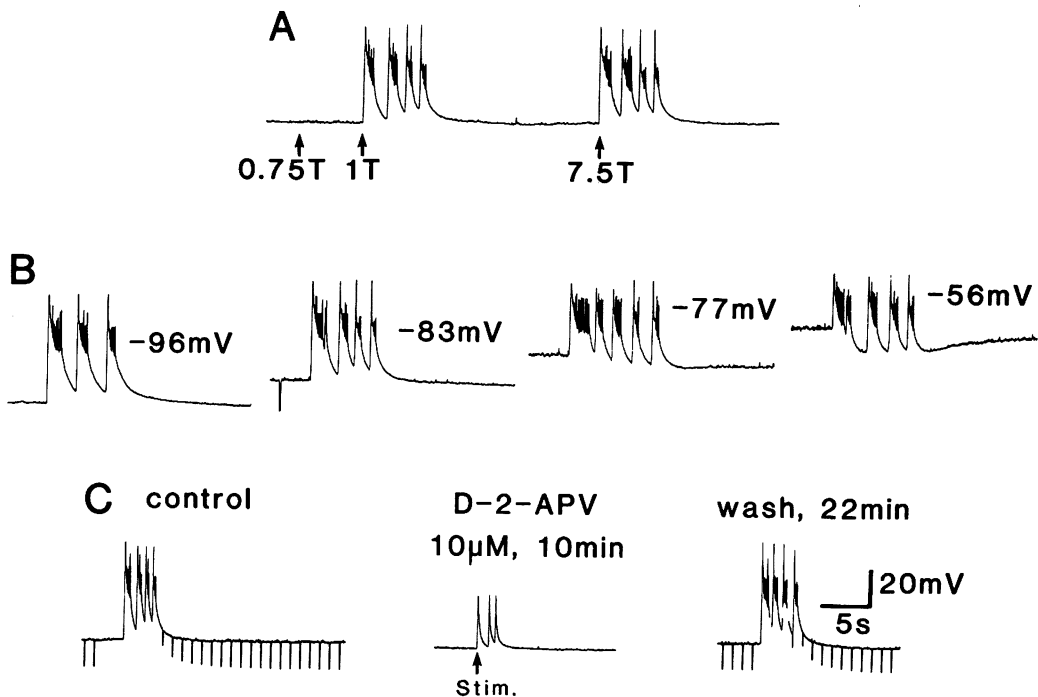


FIG. 13. Evoked and spontaneous epileptiform burst discharges in the absence of  $Mg^{2+}$  ions. This neuron ( $RMP = -83$  mV) was recorded in a slice kept for 4 h in a  $Mg^{2+}$ -free solution. *A*: all-or-nothing characteristics of evoked epileptiform discharges. The stimulus intensity necessary to evoke a burst discharge was termed threshold intensity,  $T$ . A stimulus with an intensity of 0.75 T was not effective, whereas a 10-fold increase in stimulus strength (to 7.5 T) did not enhance the response. The time points of stimulation are indicated by the arrows. Action potentials are cut off due to the limited frequency response of the chart writer. *B*: spontaneous epileptiform activity recorded in the absence of  $Mg^{2+}$  at different membrane potentials. Note the changes in the amplitudes of the individual bursts following changes in the membrane potential. *C*: effect of D-2-APV (10  $\mu$ M, 10 min) on spontaneous epileptiform burst discharges. The antagonist reversibly blocked the spontaneous activity and reduced the amplitude of the evoked discharges (compare *C*, center and *A*, 1 T).

in an increase and a decrease, respectively, of the burst amplitude (Fig. 13*B*). Furthermore, these bursts were found to be reversibly blocked by D-2-APV (5–20  $\mu$ M) added to the bathing medium (Fig. 13*C*), suggesting an involvement of NMDA receptors in their generation. In the absence of  $Mg^{2+}$  ions, D-2-APV had no effect on membrane potential,  $R_N$ , or rheobase current.

When  $Mg^{2+}$  ions were reintroduced, qualitatively normal postsynaptic potentials could be recorded, even after very long incubation periods in solutions without  $Mg^{2+}$  ions. Figure 14 depicts postsynaptic potentials recorded 13 min following the addition of  $Mg^{2+}$  ions to the bathing solution after a 4-h exposure to magnesium-free saline

(same neuron as Fig. 13). At a low-stimulus intensity (11 nC), an eEPSP was evoked (Fig. 14, left). Upon an increase to 14 nC, the neuron responded with an eEPSP followed by a large amplitude IEPSP (Fig. 14, left). This large IEPSP disappeared upon stimulation with an intensity which produced chloride- and potassium-dependent IPSPs (Fig. 14, center and right) as described previously (29).

## DISCUSSION

The present experiments investigated the validity of two predictions (29) concerning the generation of eEPSPs in rat neocortical neurons. In addition, we examined the involve-

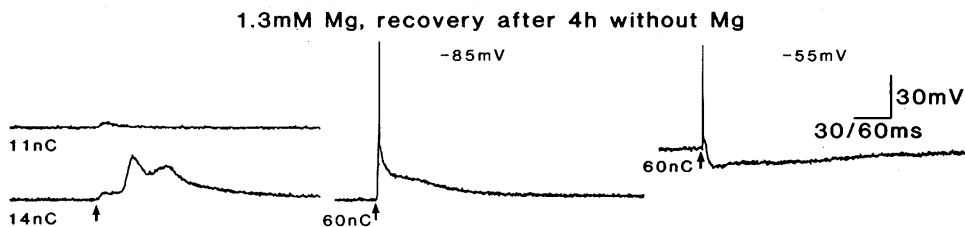


FIG. 14. Reversibility of the effects of a 4-h reduction in  $[Mg^{2+}]_0$ . Same neuron as in Fig. 12. Upon an increase in  $[Mg^{2+}]_0$  to 1.3 mM, the membrane potential hyperpolarized to  $-85$  mV. A stimulus with an intensity of 11 nC evoked an eEPSP (left panel, upper trace). Increasing the stimulation strength to 14 nC resulted in the elicitation of an eEPSP followed by a IEPSP (left panel, lower trace). The threshold intensity was found to be 60 nC (center). To this intensity the neuron responded with an suprathreshold EPSP followed by a depolarizing IPSP as verified by depolarizing the membrane potential to  $-55$  mV (right).

ment of NMDA receptors in the induction of LTP in neocortical neurons *in vitro*. On the basis of the electrophysiological properties of the eEPSP, we proposed that it is generated at synapses remote from the soma and that the changes in eEPSP waveform seen with membrane potential shifts are due to the activation or inactivation of voltage-dependent conductances rather than due to the activation of synaptic NMDA receptors (29). As a consequence, the eEPSP and its changes in waveform following changes in membrane potential should be insensitive to the selective and competitive NMDA antagonist D-2-APV, and alterations in the neuron's *I-V* relationship induced by an ion-channel blocker should lead to parallel changes in the relationship between eEPSP waveform and membrane potential.

#### *Mechanism of eEPSP generation*

Our results show that the eEPSP was not affected by D-2-APV, either at RMP or following shifts in the membrane potential. D-2-APVs lack of effect on the eEPSP cannot be attributed to an unequal distribution of the antagonist in the slice tissue, since it was added to the bathing solution at relatively high concentrations (10–20  $\mu\text{M}$ ) for long periods of time (up to 30 min). Furthermore, under the same conditions, the neuron's response to iontophoretically applied NMDA was reversibly blocked. Although the location and distribution of NMDA receptors on the surface membrane of neocortical neurons are not known, we speculate that these receptors are located predominantly at dendritic sites. In our experimental arrangement, the micropipette used to apply NMDA was positioned proximal to the recording electrode. It is reasonable to assume that the recording electrode primarily impaled neuronal somata and that therefore NMDA was delivered predominantly to the somatic area of the neuron's membrane. The slow onset of the NMDA-evoked depolarizations may be a result of a slow, depolarization-induced release from the voltage-dependent block imposed on NMDA channels by magnesium ions, or, more likely, may reflect the diffusion time necessary for the applied NMDA molecules to reach their dendritic receptors. Assuming that NMDA receptors are located on dendrites and that the eEPSP is generated by an NMDA-dependent mechanism at synapses in the same area, it should have been possible to suppress the eEPSP as well as the neuron's response to iontophoretically applied NMDA. One possible explanation of the failure of D-2-APV to block the eEPSP is that the antagonist was inaccessible to synaptic NMDA receptors. Although this possibility cannot be ruled out, it seems unlikely, and we conclude that NMDA receptors are not involved in the generation of the eEPSP.

To investigate the validity of our second prediction, it was necessary to use substances that would not interfere with the generation of the eEPSP but would significantly change the neuron's *I-V* relationship. Connors and Prince (4) showed that the lidocaine derivative QX-314 depresses the sodium conductance underlying the fast action potential. In addition, it suppresses a voltage-dependent, noninactivating sodium conductance that has been shown to produce, at least in part, depolarizing inward rectification

in hippocampal (12) and neocortical (3, 24, 25, 31) neurons. Connors and Prince (4) also showed that QX-314 affected neither the stimulus-evoked EPSP nor the glutamate-evoked depolarization recorded in hippocampal CA1 neurons. In contrast, Puil and Carlen (22) reported that another lidocaine derivative, QX-222, had a depressant action on EPSPs and glutamate-induced depolarizations in CA1 pyramidal cells of the hippocampus. However, the latter effect may result from a simultaneous reduction in depolarizing inward rectification, which, in part, determines the amplitude and resistance changes observed during depolarizations produced by iontophoretically applied glutamate (9). The results of our experiments agree with those of studies performed in hippocampal (4) and neocortical neurons (3, 24, 31). After injection of QX-314, both the generation of fast action potentials and depolarizing inward rectification were suppressed, whereas hyperpolarizing inward rectification was unaltered. Under these conditions, the eEPSPs evoked at RMP by low-intensity stimulation did not differ from those recorded in control cells, indicating that the generation mechanism was probably not affected by QX-314. However, upon depolarization, a considerable decrease in eEPSP amplitude was observed. This finding suggests a relationship between the shape of the eEPSP waveform at different membrane potentials and the *I-V* characteristics of the neurons.

Further support for this suggestion came from experiments in which cesium ions were used to block hyperpolarizing inward rectification (anomalous rectification). In mammalian neurons, cesium ions added to the extracellular solution have been shown to block both a fast anomalous rectifying conductance (5) and a slow anomalous rectifier (6, 10, 13, 14, 23). The increase in the slope of the hyperpolarizing *I-V* curve observed in our experiments after the application of cesium ions demonstrates the existence of similar anomalous rectifying conductances in rat neocortical neurons. Furthermore, it seems that these anomalous rectifiers are well expressed in rat neocortical neurons, since they are strong enough to shunt the amplitudes of eEPSPs and IEPSPs. In the presence of cesium, the amplitude of the eEPSP increased with hyperpolarization, and large-amplitude IEPSPs could be evoked at very negative membrane potentials using relatively low stimulation intensities. The physiological significance of anomalous rectifying conductances in neocortical neurons might be the regulation of excitatory synaptic input.

In summary, we were able to provide evidence supporting the validity of two predictions we made on the basis of a hypothesis formulated in the preceding paper (29). We found that at every membrane potential tested, the eEPSP was insensitive to the selective and competitive NMDA antagonist D-2-APV. Furthermore, we demonstrated the occurrence of parallel changes in the shape of the eEPSP waveform at different membrane potentials and in the neuron's *I-V* relationship upon blockade of voltage-dependent conductances. These findings strongly support the hypothesis that the eEPSP is generated at synapses remote from the soma by an NMDA-independent mechanism and that the changes in the waveform seen with membrane potential shifts are primarily determined by the nonlinear properties of the neuron's membrane.

### *Alterations in $[Mg^{2+}]_0$*

Evidence concerning the effects of changes in  $[Mg^{2+}]_0$  on eEPSPs proved difficult to obtain under our experimental conditions. Alterations in  $[Mg^{2+}]_0$  led to a variety of effects on EPSPs and IPSPs and intrinsic membrane properties of rat neocortical neurons. It is not possible to ascribe all these effects to a  $Mg^{2+}$ -induced blockade of the conductance activated via NMDA receptors ( $g_{NMDA}$ ). As described above,  $g_{NMDA}$  is not involved in the generation of the eEPSP and is not likely to participate in the production of chloride- and potassium-dependent IPSPs. Since an increase in  $[Mg^{2+}]_0$  affected both EPSPs and IPSPs, one has to assume a general effect of  $Mg^{2+}$  ions on synaptic transmission. Furthermore, in our experiments the increase in  $[Mg^{2+}]_0$  was not compensated for by omitting an equivalent concentration of  $Ca^{2+}$  ions, resulting in a significant increase in the total extracellular concentration of divalent cations. This certainly affects the membrane surface charge screening (11), with the result of a general decrease in direct and synaptic excitability. Of course, on the assumption of an endogenous glutaminergic tonus mediated via NMDA receptors, increases in  $[Mg^{2+}]_0$  would produce an additional reduction in neuronal excitability.

Decreases in  $[Mg^{2+}]_0$  to nominally 0 mM also had multiple effects not attributable to a simple interaction between  $Mg^{2+}$  ions and  $g_{NMDA}$ . Since D-2-APV depressed the spontaneous epileptiform burst discharges, it is reasonable to assume that these bursts are mediated by the activation of NMDA receptors. However, since the selective NMDA antagonist D-2-APV did not alter intrinsic properties of the neurons, neither in the presence nor the absence of  $Mg^{2+}$  ions, increases in an endogenously excitatory tonus mediated via NMDA receptors cannot account for the alterations in intrinsic electrophysiological properties observed following the removal of  $Mg^{2+}$  ions from the bathing medium. As described above, both the antagonistic effects of  $Mg^{2+}$  ions on  $Ca^{2+}$  conductances and the change in the membrane surface charge screening have to be considered. Removal of  $Mg^{2+}$  ions from the bathing solution without substitution by other divalent cations may enhance  $Ca^{2+}$  conductances and it certainly reduces the membrane surface charge screening. Both effects lead to an increase in neuronal excitability. Upon an equimolar replacement of  $Mg^{2+}$  ions by  $Ca^{2+}$  ions, the hyperexcitability induced by removing  $Mg^{2+}$  should be less expressed. Mody et al. (18) have in fact shown that the spontaneous activity induced by removal of  $Mg^{2+}$  ions is suppressed by raising the extracellular  $Ca^{2+}$  concentration.

In summary, we were not able to provide evidence for the validity of our third prediction that the voltage-dependence of the eEPSP amplitude should remain unaltered following changes in  $[Mg^{2+}]_0$ . However, due to the multiple and unselective effects observed following changes in  $[Mg^{2+}]_0$ , we think that, at least in a slice preparation, the sensitivity to  $Mg^{2+}$  ions is not a useful tool to classify excitatory postsynaptic potentials.

### *Involvement of NMDA receptors in IEPSP and LTP*

The investigation of the involvement of NMDA receptors in the induction of LTP in neocortical neurons re-

vealed that the IEPSP itself is sensitive to the NMDA antagonist D-2-APV, although the voltage dependence of the IEPSP amplitude did not agree with an NMDA-mediated mechanism. There are several possibilities to explain this phenomenon. First, it could be assumed that the NMDA receptors responsible for the D-2-APV sensitivity of the IEPSP are not located on the neuron recorded but on a presynaptic locally projecting neuron. When an excitation occurred that involved the activation of NMDA receptors, this neuron would release an excitatory transmitter, generating an EPSP in the postsynaptic neuron by an NMDA receptor-independent, "conventional" mechanism. In this case, D-2-APV would produce a disinhibition by inhibition of an excitatory interneuron. A similar disinhibitory effect would occur as a result of an intrinsic inhibitory influence on excitatory local circuit neurons. In fact, intracellular recordings from the cat sensorimotor cortex *in vivo* provided evidence for the existence of such disinhibitory events following electrical stimulation of the caudate nucleus (36). Second, NMDA receptors responsible for the D-2-APV sensitivity of the IEPSP might be located on the postsynaptic neuron, and, instead of mediating the EPSP, would modulate its amplitude upon activation. Assuming that the NMDA receptors were present as extrasynaptic receptors close to the synapse generating the EPSP by a "conventional" mechanism (e.g., activation of quisqualate/kainate receptors by L-glutamate), a "spillover" of the transmitter would activate the extrasynaptic NMDA receptors. The result would be a membrane area displaying a predominantly negative slope conductance, which, in turn, would amplify the amplitude of the EPSP. Since NMDA receptors are involved, D-2-APV would block such an amplification. Third, NMDA receptors might be present on the presynaptic terminals. Activation of these receptors would increase the amount of excitatory transmitter released. However, this mechanism seems unlikely, since there is no morphological evidence for asymmetrical, i.e., presumably excitatory, axoaxonal synapses (21).

From our experiments, we assume that the IEPSP is generated by a polysynaptic pathway and that the NMDA receptors responsible for the D-2-APV sensitivity of the IEPSP are located on excitatory local circuit neurons presynaptic to the neuron recorded. This conclusion is supported by the inability of the IEPSP to follow stimulation frequencies  $> 0.5$  Hz (29) and by the fact that LTP of the IEPSP can be induced by using stimulus intensities that do not evoke a detectable postsynaptic response in the recorded neuron (29). On the assumption of postsynaptic, extrasynaptic NMDA receptors both features of the IEPSP would be difficult to explain. In this case, an apparent frequency-dependent depression of the IEPSP might occur due to a very rapid desensitization or tachyphylaxis of NMDA receptors. However, with the application protocol used in this study, there was no evidence of a desensitization of the neuron's response to iontophoretically applied NMDA (see also Ref. 33). Furthermore, the very rapid reversal of the IEPSP argues against a desensitization or tachyphylaxis. In addition, if activation of NMDA receptors is necessary to induce LTP, and our results provided evidence for this, and if NMDA receptors are located on the postsynaptic neuron, it should have been impossible to

induce LTP by using stimulus intensities that did not evoke a postsynaptic response, since these stimulus strengths were far below the activation threshold for D-2-APV-sensitive IEPSPs.

In the light of the D-2-APV sensitivity of the IEPSP, we expected to be able to block the induction of LTP by application of D-2-APV. Since we suggested that the NMDA receptors involved in LTP are located on presynaptic excitatory cells, we must conclude that the primary process leading to LTP of the IEPSP did not occur in the postsynaptic neuron. The enhanced amplitude of the IEPSP recorded in the postsynaptic neuron was an expression of LTP in local circuit neurons.

QX-314 was a generous gift from Astra Pharmaceutical. This work was supported by National Institute of Neurological and Communicative Disorders and Stroke Grants NS-22373 and NS-18145, by Deutsche Forschungsgemeinschaft Grant Su 104/1-1, and by a Fellowship Award from the Max Kade Foundation to B. Sutor.

Present address of B. Sutor: Physiologisches Institut der Universität, Pettenkoferstrasse 12, 8000 München 2, FRG.

Address for reprint requests: J. Hablitz, Department of Physiology and Biophysics, Neurobiology Research Center, University of Alabama at Birmingham, Birmingham, AL 35294.

Received 21 July 1988; accepted in final form 21 October 1988.

## REFERENCES

- ARTOLA, A. AND SINGER, W. Long-term potentiation and NMDA receptors in rat visual cortex. *Nature* 330: 649–652, 1987.
- COLLINGRIDGE, G. L., KEHL, S. J., AND McLENNAN, H. Excitatory amino acids in synaptic transmission in the Schaffer collateral commissural pathway of the rat hippocampus. *J. Physiol. Lond.* 334: 33–46, 1983.
- CONNORS, B. W., GUTNICK, M. J., AND PRINCE, D. A. Electrophysiological properties of neocortical neurons in vitro. *J. Neurophysiol.* 48: 1302–1320, 1982.
- CONNORS, B. W. AND PRINCE, D. A. Effects of local anesthetic QX-314 on the membrane properties of hippocampal pyramidal neurons. *J. Pharmacol. Exp. Ther.* 220: 476–481, 1982.
- CONSTANTI, A. AND GALVAN, M. Fast inward-rectifying current accounts for anomalous rectification in olfactory cortex neurones. *J. Physiol. Lond.* 335: 153–178, 1983.
- CREPEL, F. AND PENIT-SORIA, J. Inward rectification and low-threshold calcium conductance in rat cerebellar Purkinje cells. An in vitro study. *J. Physiol. Lond.* 372: 1–23, 1986.
- FLATMAN, J. A., SCHWINDT, P. C., AND CRILL, W. E. The induction and modification of voltage-sensitive responses in cat neocortical neurons by N-methyl-D-aspartate. *Brain Res.* 363: 62–77, 1986.
- HABLITZ, J. J. Action of excitatory amino acids and their antagonists on hippocampal neurons. *Cell. Mol. Neurobiol.* 5: 389–405, 1985.
- HABLITZ, J. J. AND LANGMOEN, I. A. Excitation of hippocampal pyramidal cells by glutamate in the guinea-pig and rat. *J. Physiol. Lond.* 325: 317–331, 1982.
- HALLIWELL, J. V. AND ADAMS, P. R. Voltage-clamp analysis of muscarinic excitation in hippocampal neurons. *Brain Res.* 250: 71–92, 1982.
- HILLE, B. *Ionic Channels of Excitable Membranes*, Sunderland, MA: Sinauer, 1984.
- HOTSON, J. R., PRINCE, D. A., AND SCHWARTZKROIN, P. A. Anomalous inward rectification in hippocampal neurons. *J. Neurophysiol.* 42: 889–895, 1979.
- KUBOTA, M., NAKAMURA, M., AND TSUKAHARA, N. Ionic conductance associated with electrical activity of guinea-pig red nucleus neurones in vitro. *J. Physiol. Lond.* 362: 161–171, 1985.
- MAYER, M. L. AND WESTBROOK, G. L. A voltage-clamp analysis of inward (anomalous) rectification in mouse spinal sensory ganglion neurones. *J. Physiol. Lond.* 340: 19–45, 1983.
- MAYER, M. L. AND WESTBROOK, G. L. The action of N-methyl-D-aspartic acid on mouse spinal neurones in culture. *J. Physiol. Lond.* 361: 65–90, 1985.
- MAYER, M. L. AND WESTBROOK, G. L. The physiology of excitatory amino acids in the vertebrate central nervous system. *Prog. Neurobiol.* 28: 197–276, 1987.
- MAYER, M. L., WESTBROOK, G. L., AND GUTHRIE, P. B. Voltage-dependent block by Mg<sup>2+</sup> of NMDA responses in spinal cord neurones. *Nature Lond.* 309: 261–263, 1984.
- MODY, I., LAMBERT, J. D. C., AND HEINEMANN, U. Low extracellular magnesium induces epileptiform activity and spreading depression in rat hippocampal slices. *J. Neurophysiol.* 57: 869–888, 1987.
- MONAGHAN, D. L. AND COTMAN, C. W. Distribution of N-methyl-D-aspartate-sensitive L-[<sup>3</sup>H]glutamate-binding sites in rat brain. *J. Neurosci.* 5: 2909–2919, 1985.
- NOWAK, L., BREGESTOVSKI, P., ASCHER, P., HERBET, A., AND PROCHIANTZ, A. Magnesium gates glutamate-activated channels in mouse central neurones. *Nature Lond.* 307: 462–465, 1984.
- PETERS, A. Synaptic specificity in the rat cerebral cortex. In: *Synaptic Function*, edited by G. M. Edelman, W. E. Gall, and W. M. Cowan. New York: Wiley, 1987, p. 373–397.
- PUIL, E. AND CARLEN, P. L. Attenuation of glutamate-action, excitatory postsynaptic potentials, and spikes by intracellular QX-222 in hippocampal neurons. *Neuroscience* 11: 389–398, 1984.
- SPAIN, W. J., SCHWINDT, P. C., AND CRILL, W. E. Anomalous rectification in neurons from cat sensorimotor cortex in vitro. *J. Neurophysiol.* 57: 1555–1576, 1987.
- STAFSTROM, C. E., SCHWINDT, P. C., CHUBB, M. C., AND CRILL, W. E. Properties of persistent sodium conductance and calcium conductance of layer V neurons from cat sensorimotor cortex in vitro. *J. Neurophysiol.* 53: 153–170, 1985.
- STAFSTROM, C. E., SCHWINDT, P. C., FLATMAN, J. A., AND CRILL, W. E. Properties of subthreshold response and action potential recorded in layer V neurons from cat sensorimotor cortex in vitro. *J. Neurophysiol.* 52: 244–263, 1984.
- STREIT, P. Glutamate and aspartate as transmitter candidates for systems of the cerebral cortex. In: *Cerebral Cortex. Functional Properties of Cortical Cells*, edited by E. G. Jones and A. Peters. New York: Plenum, 1984, vol. 2, p. 119–143.
- SUTOR, B. AND HABLITZ, J. J. Properties of subthreshold EPSPs in rat neocortical neurons. *Soc. Neurosci. Abstr.* 13: 156, 1987.
- SUTOR, B. AND HABLITZ, J. J. Electrophysiological properties of excitatory postsynaptic potentials in rat neocortical neurons in vitro. *Pfluegers Arch.* 411, Suppl. I: R153, 1988.
- SUTOR, B. AND HABLITZ, J. J. Excitatory postsynaptic potentials in rat neocortical neurons in vitro. I. Electrophysiological evidence for two distinct EPSPs. *J. Neurophysiol.* 61: 607–620, 1989.
- SUTOR, B., JORDAN, W., AND ZIEGLGÄNSBERGER, W. Evidence for a magnesium-insensitive membrane resistance increase during NMDA-induced depolarizations in rat neocortical neurons in vitro. *Neurosci. Lett.* 75: 317–322, 1987.
- SUTOR, B. AND ZIEGLGÄNSBERGER, W. A low-voltage activated, transient calcium current is responsible for the time-dependent depolarizing inward rectification of rat neocortical neurons in vitro. *Pfluegers Arch.* 410: 102–111, 1987.
- THOMSON, A. M. A magnesium-sensitive post-synaptic potential in rat cerebral cortex resembles neuronal responses to N-methylaspartate. *J. Physiol. Lond.* 370: 531–549, 1986.
- THOMSON, A. M. Comparison of responses to transmitter candidates at an N-methylaspartate receptor mediated synapse, in slices of rat cerebral cortex. *Neuroscience* 17: 37–47, 1986.
- THOMSON, A. M. AND LODGE, D. Selective blockade of an excitatory synapse in rat cerebral cortex by the sigma opiate cyclazocine: an intracellular in vitro study. *Neurosci. Lett.* 54: 21–26, 1985.
- THOMSON, A. M., WEST, D. C., AND LODGE, D. An N-methylaspartate receptor-mediated synapse in rat cerebral cortex: a site of action of ketamine? *Nature Lond.* 313: 479–481, 1985.
- VIETH, J., KNEISE, U., AND KAFTERLEIN, J. Evozierte Enthemmung und Bahnungsminde rung in corticale Nervenzellen. *Arch. Psychiatr. Nervenkr.* 218: 271–299, 1974.